THE JOURNAL OF PHYSICAL CHEMISTRY C

Article

pubs.acs.org/JPCC

# Crystalline Alloys of Organic Donors and Acceptors Based on TIPS-Pentacene

Jes B. Sherman,[†] Kai Moncino,[‡] Tunna Baruah,[§] Guang Wu,[†] Sean R. Parkin,[∥] Balaji Purushothaman,[∥] Rajendra Zope,[§] John Anthony,[∥] and Michael L. Chabinyc*[,‡]

[†]Department of Chemistry and Biochemistry and [‡]Materials Department, University of California Santa Barbara, Santa Barbara, California 93106, United States

[§]Department of Physics, The University of Texas at El Paso, El Paso, Texas 79968, United States

[∥]Department of Chemistry, University of Kentucky, Lexington, Kentucky 40506, United States

Supporting Information

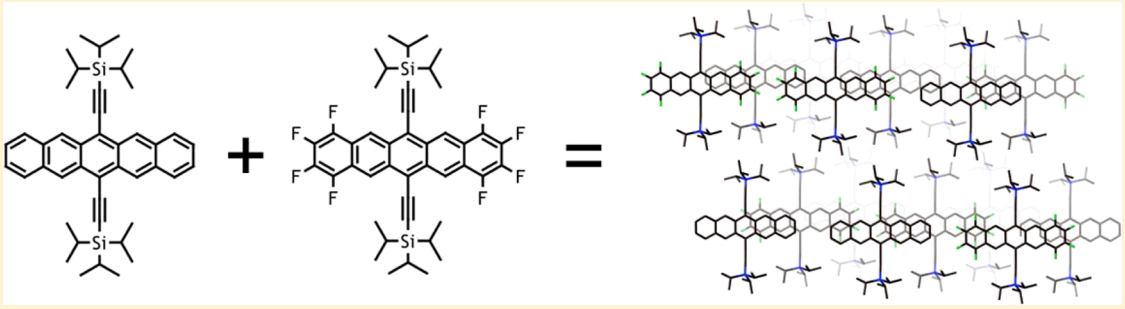


**ABSTRACT:** Co-crystals of organic semiconductors can provide model systems for the study of fundamental optoelectronic properties and also new functionality. 6,13-Bis(triisopropylsilylethynyl)pentacene (TIPS-Pn) and its fluorinated analogue 1,2,3,4,8,9,10,11-octafluoro-bis(triisopropylsilylethynyl)pentacene (F8TIPS-Pn) form crystalline substitutional alloys during bulk crystal growth from solution. Alloys can also be formed by blade casting thin films from solution. The compounds appear to have sufficient geometric similarity to be miscible in all proportions without inducing long-range disorder in the solid state. The offsets of the electronic levels of TIPS-Pn and F8TIPS-Pn in pure form are similar to those found in bulk heterojunction solar cells. UV/vis spectroscopy and density functional theory demonstrate the charge transfer absorption in the alloy crystals corresponds to an excitation across molecular pairs.

## INTRODUCTION

Organic semiconductors are frequently blended with other organic materials to form solids with functional properties, such as in blends of electron donors and acceptors that lead to bulk heterojunction solar cells.[1] More broadly, donor/acceptor (D/A) complexes of organic compounds have been studied for their unusual electronic and photophysical properties.[2] In a donor−acceptor complex, an electronic transition from a neutral D/A pair to a state with either partial or full charge transfer leads to the characteristic "charge transfer" absorption.[3] Electronic donor−acceptor interactions are particularly important in the solid state to form conductors, such as the TTF-TCNQ complex,[4,5] and recently to form mixed crystals with ambipolar charge transport.[6−8] Improving our understanding of how to control crystallization of pairs of materials and their resulting properties will help in the development of new alloys with enhanced properties for an array of applications.

Mixed crystals and co-crystals with and without charge transfer interactions have been studied to understand the fundamental processes in crystallization and to develop new functionality. In general, two organic compounds with sufficient geometric similarity are potentially miscible in the solid state and are capable of forming crystals with variable composition (referred to as either an alloy, mixed crystal, or solid solution).[9] The addition of a second component may lead to changes in crystal habit or polymorph selection, which are important considerations in pharmaceutical research.[10−12] Historically, dye inclusion crystals were useful in studying crystal growth mechanisms and solid solutions.[13] Mixed crystals may also exhibit physical properties that differ from the parent compounds; in energetic materials, the co-crystallization can lead to improved stability and safer handling.[14−16] These studies have provided significant insight into design rules to control crystallization of organic materials.

In organic electronics, the addition of a second component to form a solid solution provides a means to introduce functional guests that can act as dopants, engineered charge trapping sites, or emissive guests. Currently, the most

**Received:** July 2, 2015
**Revised:** August 14, 2015
**Published:** August 31, 2015





DOI: 10.1021/acs.jpcc.5b06363
J. Phys. Chem. C 2015, 119, 20823−20832

technologically relevant solid solutions of organic semiconductors are in organic light emitting diodes (OLEDs), where a small concentration of an emissive guest is dissolved in a conductive host matrix.[17,18] Model systems as Bridgman-grown crystals of anthracene doped with tetracene or acridine were used to determine trap levels and provide experimental support to charge transport models.[19,20] Pentacene and perfluoropentacene have been coevaporated to produce thin films to study donor−acceptor interactions and structural ordering.[21] Solution-processed thin films of substituted fluorinated anthradithiophene derivatives with various additives have been used to study photoexcited charge carrier dynamics.[22] Many of these studies include characterization of either thin films or single crystals, but rarely both. While single crystals enable structure determination, thin films are more relevant to device applications and may feature different polymorphs or disorder not observed in single crystals.[23,24]

We sought to form a mixed crystal comprising materials with offsets in electronic levels similar to those observed in well-performing organic solar cells—around 0.3 to 0.5 eV between the electron affinity of the donor and acceptor with a comparable offset in their ionization energies.[1] To this end, we have selected the organic semiconductors 6,13-bis(triisopropylsilylethynyl)pentacene (TIPS-Pn) and 6,13-1,2,3,4,8,9,10,11-octafluoro-bis(triisopropylsilylethynyl)-pentacene (F8TIPS-Pn), shown in Figure 1. TIPS-Pn has been

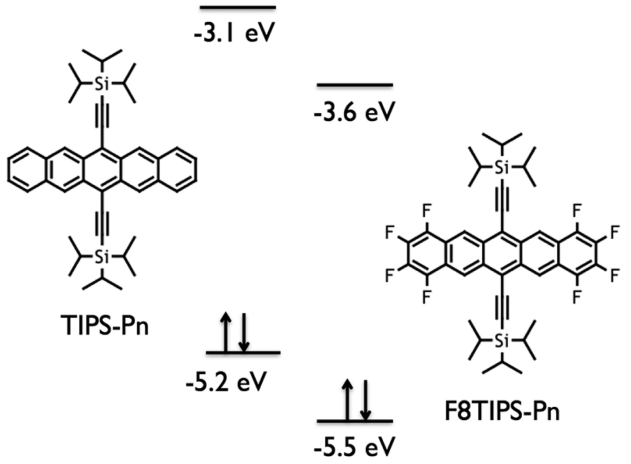


**Figure 1.** Chemical structures of TIPS-Pn and F8TIPS-Pn along with their frontier molecular orbital levels based on cyclic voltammetry data.

widely researched as a thin-film transistor material because it can be easily processed from solution, leading to thin films with high charge carrier mobility.[25] F8TIPS-Pn, an isostructural derivative, is also highly soluble and can be processed from solution, and has been investigated as an electron acceptor in solar cells.[26] We find that these materials co-crystallize into alloys efficiently, allowing for large single crystals suitable for full determination of the molecular packing structure, and they also co-crystallize in thin films.

## RESULTS AND DISCUSSION

**Alloying of TIPS-Pn and F8TIPS-Pn in Single Crystals.** The bulk structures of both TIPS-Pn and F8TIPS-Pn have been reported.[26,27] The two compounds are chemically similar, and both pack in a $\beta$-motif, in which only cofacial interactions are present between neighboring acene cores (Figure 2).[28] The

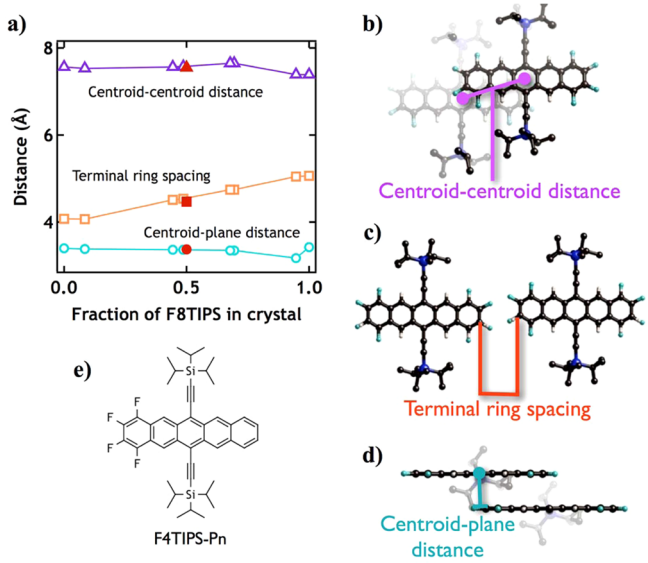


**Figure 2.** Packing parameters observed in the crystal structures are illustrated in the plot in (a). The centroid−centroid (b) and centroid−plane (d) distances show little change with F8TIPS-Pn loading. The distance between adjacent, coplanar terminal acene rings (c) increases steadily as F8TIPS-Pn loading increases. The filled red symbols correspond to distances observed in crystals of (e) F4TIPS-Pn.

largest difference between the two structures is that there are two molecules in the unit cell of F8TIPS and one in the unit cell of TIPS-Pn (Table S1). Although both are triclinic, $P\bar{1}$, an inversion center is present in the center of the single molecule in the TIPS-Pn unit cell, but the F8TIPS-Pn acene core deviates slightly from planarity. Thus, two molecules compose the F8TIPS-Pn unit cell, and the requisite inversion center for space group $P\bar{1}$ lies between them. The carbon atom density per unit cell volume is very similar for the two compounds—TIPS-Pn contains 0.046 carbon atoms per Å$^3$, and F8TIPS-Pn contains 0.045 carbon atoms per Å$^3$. We sought to determine if TIPS-Pn and F8TIPS-Pn would co-crystallize from solution, as we would expect on the basis of their structural similarity.

Slow evaporation of a chloroform solution containing TIPS-Pn and F8TIPS-Pn produced mixed crystals of sufficient size (generally, several hundred microns on a side) for structure determination using single-crystal X-ray diffraction. Pure crystals containing solely TIPS-Pn or F8TIPS-Pn were not observed after growth from a mixed solution. Changing the relative proportions of TIPS-Pn to F8TIPS-Pn allows control over the composition of the mixed crystals, but crystals grown from the same solution exhibit some variation in composition. We verified the composition of the mixed crystals by dissolution and analysis by HPLC using 10 mixed crystals from a particular growth run (this data is shown in Figure S1). We found ∼10% deviation in the fractional composition of F8TIPS from crystal to crystal; for example mixed crystals contained an average of 60% F8TIPS-Pn when the growth solution contained 50% F8TIPS-Pn. This can be attributed to the lower solubility of F8TIPS-Pn.

The single mixed crystals provided X-ray scattering data of sufficient quality to determine that the materials are random alloys. Splitting of individual reflections, which would indicate phase separation of TIPS-Pn and F8TIPS-Pn into separate domains, was not observed. Fluorine and hydrogen atoms in the terminal rings of the acene (as well as the carbon atoms to


DOI: 10.1021/acs.jpcc.5b06363
J. Phys. Chem. C 2015, 119, 20823−20832

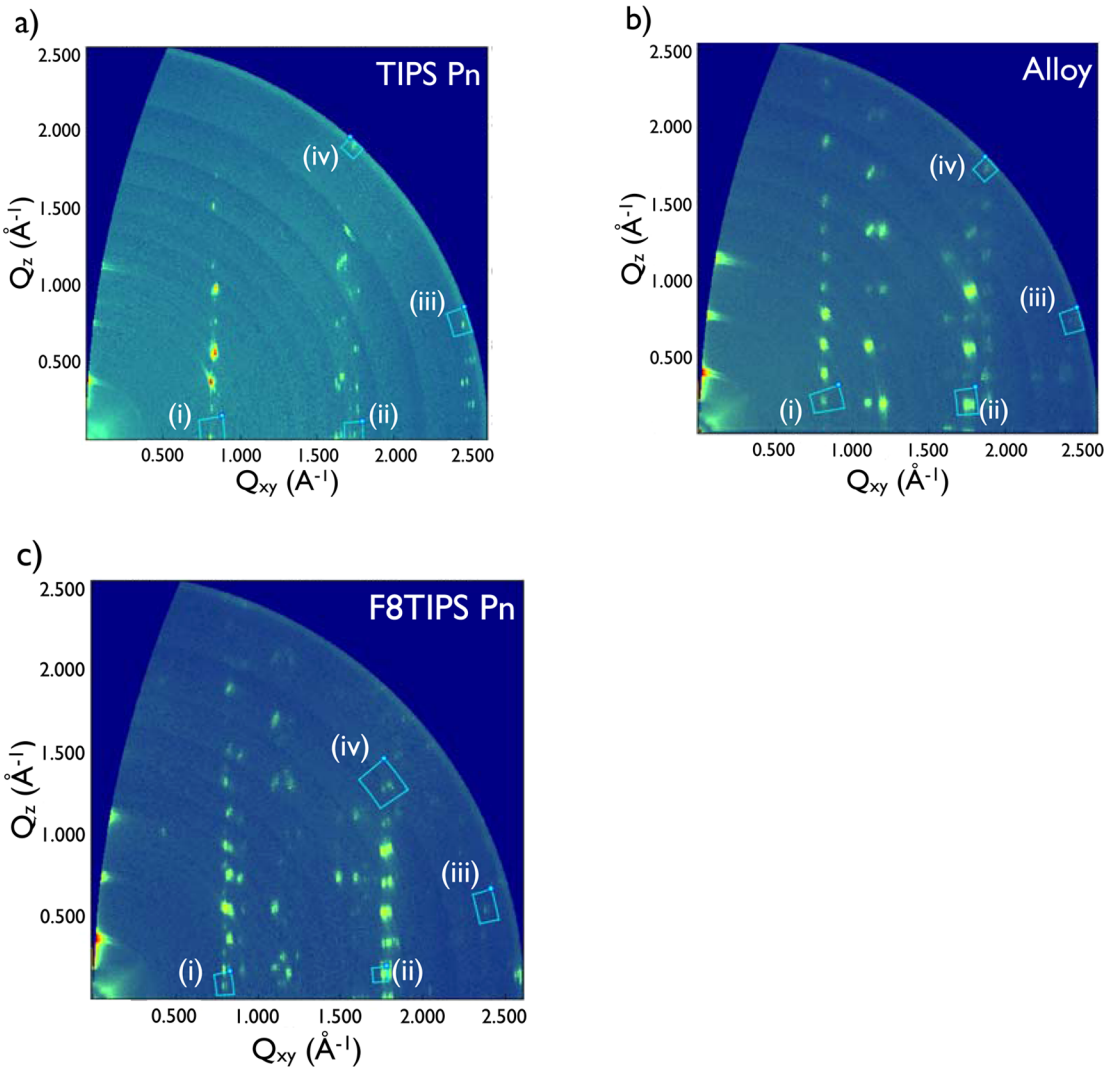


**Figure 3.** In the scattering data collected for (a) TIPS-Pn, (b) a 1:1 mixed film, and (c) F8TIPS-Pn, the positions of the four clusters of peaks indicated as *i*, *ii*, *iii* and *iv* are given in Table S3.

which fluorine and hydrogen are bonded) were assigned partial occupancy during crystal structure refinement. After refinement, the variable indicating the partial site occupancy factor for the fluorine atoms was taken to indicate the fractional composition of F8TIPS-Pn in the crystal. This value corresponded well to the NMR data (Figure S2). At very high fractional composition of F8TIPS-Pn, the molecular packing of the alloys closely resembles that observed in pure F8TIPS-Pn. As the proportion of TIPS-Pn in the crystals increases, the packing of the molecules in the alloy crystals becomes like TIPS-Pn, with one molecule in the unit cell. Rotational disorder is observed in the isopropyl groups, and refinement of the disorder reveals that a minority of the isopropyl groups occupy sites 60° from the positions in which the majority lie. At compositions with less than 50% F8TIPS content, this freedom is no longer present because the molecules pack more tightly with increased TIPS-Pn loading—that is, the unit cell volume decreases. The carbon atom density per unit cell volume of the mixed crystals is almost identical to that of the parent compounds (0.045−0.046 carbon atoms per $Å^3$).

The intermolecular interactions and packing are of interest for understanding the electronic structure of donor−acceptor interactions in solids. Benzene and perfluorobenzene are known to form complexes in the solid state.[29] Despite the fact that single crystals of benzene and single crystals of perfluorobenzene feature herringbone packing (edge-to-face interactions), mixed crystals of the two molecules exhibit only cofacial interactions, and the molecules alternate within a columnar stack.[30] This is attributed to the quadrupole moments of the two molecules, which are similar in magnitude but opposite in phase[31] by some and due to electrostatic interactions between the ring and substituent by others.[32,33] The highly electronegative fluorine substituents in perfluorobenzene withdraw electron density to the periphery of the ring; this leaves a positive electrostatic potential in the center of the ring, which interacts with the negative electrostatic potential above and below the plane of the benzene ring adjacent in the stack.[32] This alternant columnar stack motif is not limited to benzene and perfluorobenzene, but has also been observed in other mixtures of arenes and perfluoroarenes.[34,35] For example, pentacene and perfluoropentacene both crystallize with herringbone packing motifs.[36] The 1:1 mixed phase of pentacene/perfluoropentacene would be an obvious comparison for the TIPS-Pn:F8TIPS-Pn mixed crystals, but we are not aware of any reported single-crystal structures for that system.


DOI: 10.1021/acs.jpcc.5b06363
J. Phys. Chem. C 2015, 119, 20823−20832

The molecular packing of the pentacene:perfluoropentacene blend, which produces crystalline thin films, has not been characterized.

Unlike pentacene and perfluoropentacene, TIPS-Pn and F8TIPS-Pn both crystallize in a $\beta$-motif, with only cofacial $\pi-\pi$ interactions, and mixed crystals containing both TIPS-Pn and F8TIPS-Pn also exhibit this $\beta$-motif packing.[26−28] Relevant packing parameters for each structure are illustrated and plotted against F8TIPS-Pn composition in Figure 2a. The distance between the plane of one molecule and the centroid of its neighbor does not appear to change significantly as the fractional composition of F8TIPS-Pn increases (this distance varies by only 0.251 Å). Additionally, there is no trend in the distance between centroids of neighboring molecules (this distance shifts by only 0.258 Å over the series of crystal structures). The only significant difference across the series is the trend observed in the distances between carbon atoms in adjacent, coplanar terminal acene rings (illustration in Figure 2b,c,d). This distance increases by approximately 1 Å across the series of structures as F8TIPS-Pn loading increases. This is not surprising, because the van der Waals radius of fluorine is larger than that of hydrogen, and carbon−fluorine bonds are longer than carbon−hydrogen bonds.[37] Similarly, typical H and F atomic volumes calculated over about 10 000 organic crystal structures are 5.4 and 11.5 Å$^3$, respectively.[38]

A crystal structure of a tetrafluorinated TIPS pentacene derivative (F4TIPS-Pn, shown in Figure 2e), which shares some similarities with the alloy, has been reported.[26] In F4TIPS-Pn, one terminal ring of the acene core is functionalized with four fluorine atoms. Disorder around the crystallographic inversion center in the reported F4TIPS-Pn structure makes it resemble an alloy with strict 1:1 stoichiometry. The F4TIPS-Pn structure exhibits packing very similar to the alloy series, with centroid−centroid distance of 7.549 Å and a centroid−plane distance of 3.377 Å. The terminal ring spacing for the tetrafluorinated TIPS pentacene structure is 4.471 Å, slightly lower than observed in the alloy structure containing closest to 50% F8TIPS-Pn.

The electronic properties of mixed donor−acceptor crystals depend strongly on the molecular packing and stoichiometry of the crystal.[39,40] For example, there many known mixed crystals with TCNQ as an acceptor and donors, such as BED-TTFF[41] and perylene,[42] that have many polymorphic forms. Recent work on perylene:TCNQ has found that growth conditions from vapor can strongly affect composition leading to crystals with D:A ratios of 1:1, 2:1, and 3:1 with significantly different structures and transport properties.[42] Our results here differ in that we observe crystallization with varying composition rather than with fixed stoichiometries, most likely due to the structural similarity of the donor and acceptor. It is possible that under different growth conditions other structures may form, particularly in thin films.[23]

**Solution Processed Films.** Due to the interest in solution processing of thin films for organic electronics, we also sought to determine if TIPS-Pn and F8TIPS-Pn would form alloys under typical casting conditions for thin films. We chose to deposit the films using blade coating from solutions similar to those used to form the single crystals. While single crystal growth took approximately 1 week, blade coated films took less than 1 min to cast. In order to examine substitutional disorder 200in these films, we cast thin films of both materials as well as mixtures of the two. We then used synchrotron source grazing incidence wide-angle scattering (GIWAXS) with 2D detection to examine the resulting films. We note that different exposure times were used for the different samples in order to avoid saturating the detector; the short exposure times used for the TIPS-Pn film led to the higher background. Because blade coating can induce directional growth in some cases, we first measured X-ray scattering with the beam parallel to the growth direction, then rotated roughly 90° to expose with the beam perpendicular to the growth direction to verify there was no significant anisotropy. The films dried rapidly, as is evident in the optical microscope images in Figure S3, so the domains are small enough that the beam should sample many domains with a range of in-plane orientations, and thus we expect that scattering data are not biased by preferred orientation.

We analyzed the thin film scattering data for TIPS-Pn (Figure 3a), a 1:1 blend (Figure 3b), and F8TIPS-Pn (Figure 3c) using our detailed information from single crystals of TIPS-Pn and F8TIPS-Pn (Figure S4, S5, and S6). To better interpret thin film X-ray scattering data that is collected at ambient temperature, we indexed single crystals at ambient temperature. Our assumption is that the gross positions of the molecules do not change, and therefore that relative reflection intensities are what we would predict from the bulk structure (collected at cryogenic temperatures). We found subtle differences in the unit cell parameters due to the collection temperature difference, summarized in Table 1. In most cases, thermal expansion results in a small increase in unit cell volume; the $a$ axis of F8TIPS-Pn however undergoes a small negative thermal expansion, which has also been reported for pentacene.[43]

**Table 1. Unit Cell Parameters for Single Crystals at Cryogenic Temperature (~90−100 K) and Ambient Temperature (~300 K)**

| unit cell parameter | TIPS-Pn | 1:1 mixed crystal | F8TIPS-Pn |
|---|---|---|---|
| $a$ (Å) | 7.565[a]/7.71[c] | 7.649/7.68[c] | 7.718[b]/7.49[c] |
| $b$ (Å) | 7.750[a]/7.81[c] | 7.723/7.86[c] | 15.545[b]/15.58[c] |
| $c$ (Å) | 16.835[a]/16.99[c] | 16.925/17.1[c] | 16.875[b]/16.82[c] |
| $\alpha$ (deg) | 89.150[a]/88.39[c] | 89.456/76.90[c] | 102.247[b]/76.48[c] |
| $\beta$ (deg) | 78.420[a]/77.27[c] | 78.443/88.35[c] | 92.666[b]/89.56[c] |
| $\gamma$ (deg) | 83.630[a]/81.96[c] | 87.889/86.30[c] | 91.546[b]/86.47[c] |

[a]ref 19. [b]ref 20. [c]ambient temperature.

GIWAXS reveals that, as has been reported for thin films of TIPS-Pn, thin films of F8TIPS-Pn, as well as films containing TIPS-Pn: F8TIPS-Pn blends, exhibit preferred orientation in the out-of-plane direction, with (00l) planes parallel to the substrate.[44] An important consideration is that all materials used in this study crystallize in $P\bar{1}$. Due to the triclinic space group, there are no systematic absences. Many reflections correspond to $d$-spacings less than 0.05 Å$^{-1}$ apart and appear in the same spatial region of the detector, leading to significant overlap of the scattering peaks. The only progression that does not overlap with other reflections is the (00$l$) family of peaks. This direction cannot be probed by the area detector in grazing incidence geometry, so out-of-plane X-ray scattering was measured using a point detector.

The molecular packing in a thin film often differs subtly from that in the bulk single-crystal structure, particularly for TIPS-Pn.[23] Organic materials crystallize into polymorphic forms, and often, the phase observed in thin films can differ from the bulk crystal structures. Polymorphism in thin films has been reported for pentacene, perfluoropentacene, and blends of the two, as well as for TIPS-Pn.[21,45,46] Vapor-deposited thin films of


DOI: 10.1021/acs.jpcc.5b06363
J. Phys. Chem. C 2015, 119, 20823−20832

TIPS-Pn have been reported to exhibit a thin film polymorph with packing very similar to that of the bulk structure, and shear-coated thin films of TIPS-Pn have been reported to exhibit multiple polymorphs.[23,47] These polymorphs have the same packing motif and differ only slightly in their unit cell parameters. Due to such subtle differences in scattering peaks, high-resolution detection of scattering is beneficial to determine their presence.

Analysis of the (00*l*) specular scattering peaks (Figures S7 and S8) indicates that drop-cast films of TIPS-Pn, F8TIPS-Pn, and a blend thereof each contain two polymorphs. In the case of TIPS-Pn and the blend film, one polymorph can be attributed to the bulk crystal structure, but thin films of F8TIPS-Pn do not appear to crystallize with the bulk crystal structure. Scattering from the blend film does not correspond well to the thin film polymorphs observed for F8TIPS-Pn or TIPS-Pn under the same casting conditions. This is readily evident from the high-resolution in-plane scattering data in Figure S9. Due to the texture of the films, peaks in the (00*l*) progression do not overlap with any other reflections.

Because the crystallites in thin films can have a higher concentration of defects relative to single crystals, blending two materials could, conceivably, lead to long-range cumulative lattice disorder.[48] For example, in bulk heterojunction films used in organic photovoltaics, even if both components are crystalline in neat thin films, multiple phases are prevalent in the blend, and molecular ordering can be strongly affected.[49,50] The width of the scattering peaks of neat TIPS-Pn and F8TIPS-Pn films provides a baseline for comparison with the blended TIPS-Pn: F8TIPS-Pn film. There are many higher-order reflections apparent in GIWAXS in the blend (Figure 3). If significant disorder were present, we would expect to see few (if any) higher-order reflections due to broadening. Detailed analysis is complicated by the fact that all unit cells in this investigation are triclinic, and two polymorphs are present in each thin film. It is important to note that the Miller indices listed for reflections in Table S2 are estimates based on simulated scattering data using bulk unit cells at ambient temperature (Table 1). The diffraction patterns for TIPS-Pn and the mixed films correspond well to simulation, but for F8TIPS-Pn, the thin film unit cell dimensions and structure factors are significantly different. Therefore, we selected reflections for F8TIPS-Pn that were in the same region of the detector as selected reflections for TIPS-Pn and the mixed films, and that were also sufficiently intense. While we attempted to select reflections that were sufficiently isolated (according to bulk structures) to be well-resolved, the peak widths may still be overestimated, and therefore coherence lengths in Figure 4 are likely underestimated.

Analysis of peak breadth by order for reflections in selected regions of each diffraction pattern indicates that the alloy film exhibits disorder comparable to that observed in TIPS-Pn and F8TIPS. Cumulative fluctuations in lattice positions shorten the length over which the lattice is coherent; broader peaks indicate greater variation in the lattice plane parameter in a particular crystallographic direction. Different polymorphs of the same material can exhibit different coherence lengths for the same lattice plane—for example, peak breadths differ slightly for both TIPS-Pn peaks in region B, which we believe to be the (211) reflections for the bulk phase and the thin film polymorph. In region *i* of the scattering pattern (Figure 3), the peak widths for the alloy film are slightly broader than those observed for TIPS-Pn or F8TIPS-Pn (Table S2). In regions *ii*, *iii*, and *iv*, however,

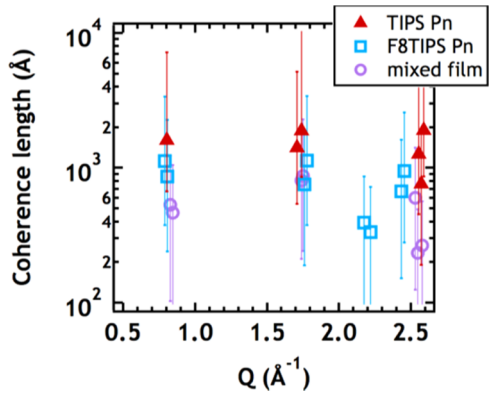


**Figure 4.** Coherence lengths for mixed films, based on in-plane peak widths, generally fall within uncertainty ranges for TIPS-Pn and F8TIPS-Pn.

the alloy film exhibits coherence lengths on the same order as F8TIPS-Pn. Only one reflection was observed for TIPS-Pn in regions *i* (010) and *iii* (032), although we do also expect to see a second peak contributed by the other polymorph—we are unable to resolve these reflections. Uncertainty in peak fitting arises when reflections overlap significantly, as is the case here. From variation in fwhm from repeatedly fitting the same two overlapping peaks, we can establish that coherence lengths for the alloy are not significantly different than those for TIPS-Pn and F8TIPS-Pn—they are within uncertainty. This is not surprising, given that we were able to grow mixed crystals with a wide range of F8TIPS-Pn composition.

In contrast with TIPS-Pn:F8TIPS-Pn blends, pentacene:perfluoropentacene thin films have been reported to grow as mixed phases with strict 1:1 stoichiometry.[45,51] Co-deposited pentacene:perfluoropentacene thin films exhibit more microstrain and smaller island sizes than films of the neat materials.[21,45] Additionally, the low intensity of the higher-order reflections and the breadth of the in-plane scattering peaks suggest that long-range order is perturbed.[45] By contrast, our results show similar coherence lengths (within experimental error) for TIPS-Pn, F8TIPS-Pn, and mixed films. The bulky TIPS substituents give TIPS-Pn and F8TIPS-Pn a higher degree of isostructurality than pentacene and perfluoropentacene. Increased geometric similarity should lead to less perturbation of long-range order in mixed TIPS-Pn:F8TIPS-Pn films, and the two compounds should be miscible over a greater composition range than pentacene:perfluoropentacene.[9]

An analysis of molecular geometry with respect to packing, conducted using the XPac software, confirms this suspicion with a quantitative dissimilarity index.[52] The dissimilarity index compares the angles and interplanar spacings between two or more crystal structures, and returns a value near 0 in the case of isostructurality. Polymorphs with similar packing often dissimilarity indices on the order of 10 or lower; compounds in which significant geometric differences (such as large vs small substituent size) exhibit large dissimilarity indices, if any similarity can be found at all.[52,53] Comparing the 22 carbon atoms in the acene core of TIPS-Pn and F8TIPS-Pn using XPac returns a dissimilarity index of 4.0, whereas comparing the same 22 carbon atoms between pentacene and perfluoropentacene yields a large dissimilarity index of 12.5. The van der Waals radius of fluorine is larger than that of hydrogen, and the C−F bond is longer than the C−H bond. However, pentacene and perfluoropentacene are smaller molecules than their silylethy-


DOI: 10.1021/acs.jpcc.5b06363
J. Phys. Chem. C 2015, 119, 20823−20832

nylated counterparts; the TIPS substituents in TIPS-Pn and F8TIPS-Pn impart so much volume that structural differences resulting from the substitution of fluorine for hydrogen have much less impact on packing.

**Electronic Structure of Donor−Acceptor Alloys.** The electronic interactions between TIPS-Pn and F8TIPS-Pn are expected to influence optical properties in the bulk crystals and thin films. Photoluminescence is a good probe of charge transfer interactions, as reported previously for Pn/FPn.[54] Unfortunately, TIPS-Pn is not strongly photoluminescent in the solid state.[22] F8TIPS-Pn suffers the same problem in the solid state, and also has a fluorescence quantum yield below the detection limit of our equipment, even when measurements on thin films are conducted with the aid of an integrating sphere. These limitations leave UV/vis spectroscopy as the best method for probing electronic interactions between the two compounds.

UV−vis spectroscopy provides further evidence for mixing, rather than phase separation, of TIPS-Pn and F8TIPS-Pn in thin films. The spectra indicate that the absorption edges of the mixed films (1.53 eV for the 1:1 blend) were slightly red-shifted relative to the absorption edges of TIPS-Pn (1.62 eV) and F8TIPS-Pn (1.72 eV) films (Figure 5a). Absorption below 1.6 eV for the mixed film could indicate photoexcitation of a charge transfer transition from TIPS-Pn to F8TIPS-Pn, based on the CV-determined HOMO and LUMO levels of TIPS-Pn and F8TIPS-Pn (Figure 5b). This is thought to result from through-space electronic interactions between adjacent TIPS-Pn and F8TIPS-Pn molecules that perturb the frontier molecular orbital energy levels. It is also important to note that, as shown in Figure S11, the mixed film spectra did not fit any linear combination of TIPS-Pn and F8TIPS-Pn spectra, which provides further evidence for homogeneous mixing of the two molecules, rather than phase separation of domains, within the thin films. Comparable shifts in the optical spectra have been observed in 1:1 co-crystals of distyrylbenzene derivatives.[6]

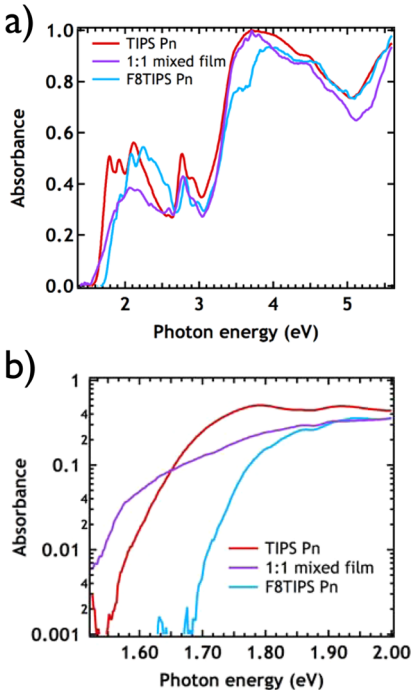


**Figure 5.** UV−vis spectra of thin films (a) shows that the absorption edge (b) of the 1:1 mixed film is red-shifted relative to TIPS-Pn and F8TIPS-Pn. Spectra of films containing different ratios of TIPS-Pn and F8TIPS-Pn are shown in Figure S10 and S11.

Donor−acceptor co-crystals may exist as either ionic or neutral structures with mixed stack crystals tending to the neutral form and side-by-side layers tending to the ionic form (charge transfer salts).[39] The slip-stacked structure here is essentially a mixed stack donor−acceptor structure. The transition from neutral to ionic form has been shown to depend on (IE − EA) − $E_M$, where $E_M$ is the Madelung energy for the crystal structure.[55,56] In the case here, the (IE − EA) is large, ∼1.7 eV, but we do observe significant change in the optical absorption with a weak charge-transfer band. Charge transfer bands with small oscillator strengths are common at organic interfaces in solar cells that have weakly electronically coupled donors and acceptors with similar energetic offsets.[57,58]

To further understand the electronic interactions in the alloy crystal, we have used a cluster model to simulate the 1:1 alloy of TIPS-Pn and F8TIPS-Pn using density functional theory (DFT). The model places TIPS-Pn and F8TIPS-Pn with a separation of 3.4 Å and a shift of 6.7 Å along the molecular axis and also by 0.71 Å laterally as seen in experimental structure. The dimer was further optimized using DFT methods at the all-electron level with Perdew−Burke−Ernzerhof exchange correlation functional.[59] These calculations are done using the NRLMOL code, which uses a large Gaussian basis set optimized for the PBE functional.[60−63] The basis set satisfies the $Z^{10/3}$ theorem that is necessary for chemically accurate converged core-level energies and is expected to provide energies that are close to converged numerical energies.[64]

We have computed the total energies of the ionic clusters at the geometry of the neutral clusters to study the quasi-particle (QP) gaps. These results are presented in Table 3. In the TIPS-Pn:F8TIPS-Pn alloy dimer, the vertical ionization energy is only 0.07 eV less than that of a TIPS-Pn molecule, and similarly the vertical electron affinity is 0.04 eV higher than for a F8TIPS-Pn molecule. These values are obtained in the gas

**Table 2. HOMO and LUMO Levels from Solution Electrochemical Measurements (Cyclic Voltammetry) vs Optical Gap Measured by Thin Film UV−vis[26]**

| material | IE (CV) | EA (CV) | IE − EA | optical gap (UV−vis) |
|---|---|---|---|---|
| TIPS-Pn | 5.2 eV | 3.1 eV | 2.1 eV | 1.6 eV |
| F8TIPS-Pn | 5.5 eV | 3.6 eV | 1.9 eV | 1.7 eV |
| alloy | 5.2 eV (TIPS) | 3.6 eV (F8) | 1.6 eV | 1.5 eV |

**Table 3. Vertical Ionization Potential (vIP), Vertical Electron Affinity (vEA), and Quasi-Particle (QP) Gaps of TIPS Monomer, Dimer, Trimers, and Tetramers**

| cluster | vIP (eV) | vEA (eV) | QP (eV) |
|---|---|---|---|
| TIPS-Pn | 5.97 | 2.01 | 3.96 |
| F8TIPS-Pn | 6.45 | 2.51 | 3.94 |
| TIPS-Pn:TIPS-Pn dimer | 5.53 | 2.43 | 3.10 |
| F8TIPS-Pn:F8TIPS-Pn dimer | 6.02 | 2.91 | 3.11 |
| TIPS-Pn:F8TIPS-Pn dimer | 5.90 | 2.55 | 3.36 |
| TIPS-Pn:F8TIPS-Pn:TIPS-Pn trimer | 5.45 | 2.78 | 2.67 |
| F8TIPS-Pn:TIPS-Pn:F8TIPS-Pn trimer | 5.57 | 2.96 | 2.71 |
| Tetramer | 5.40 | 2.98 | 2.42 |
| Expt. | 5.2 | | 2.1 |


DOI: 10.1021/acs.jpcc.5b06363
J. Phys. Chem. C 2015, 119, 20823−20832

phase and therefore differ from the experimental values obtained with cyclic voltammetry measurements where solvent stabilizes the ions. In this dimer the HOMO and LUMO are localized on the TIPS-Pn and F8TIPS-Pn components. The quasi-particle gap in the dimer is 3.36 eV at the PBE level (Table 3). To examine whether the dimer shows evidence of charge transfer, we used a Voronoi scheme,[65] which splits the molecular volume into atomic volumes, natural population analysis (NPA),[66] and a fragment charge decomposition scheme where the total molecular orbital is expressed as a combination of constituent fragment orbitals.[67] All of these schemes show very little charge transfer from TIPS-Pn to F8TIPS-Pn (0.025 e from Voronoi and 0 from NPA, 0.01 e from fragment analysis using both the NRLMOL and Gaussian09 codes).

The polarization due to the surrounding molecules in the solid state will affect the energy levels and we studied the impact of this deficiency in the dimer model using large clusters. In general, the polarization effect tends to increase the electron affinity and lower the ionization energy. To gauge the effect of neighboring molecules, we have computed the quasi-particle gaps to see its trend as the cluster size increases. The ionization energy of the pure TIPS-Pn dimer is reduced and similarly the electron affinity of the pure F8TIPS-Pn dimer increases compared to the monomers (Table 3). Similar trends are also seen in TIPS-Pn:F8TIPS-Pn:TIPS-Pn and F8TIPS-Pn:TIPS-Pn:F8TIPS-Pn trimers, as well as in a TIPS-Pn:F8TIPS-Pn:TIPS-Pn:F8TIPS-Pn tetramer. For the tetramer the QP gap reduces to 2.42 eV. These calculations show the effect of the intermolecular interactions in the pentacene alloys and highlight the necessity to consider larger cluster models.

We have further calculated the singlet excitation energies of the TIPS-Pn:F8TIPS-Pn alloy dimer using the time-dependent DFT (TDDFT) method as implemented in the Gaussian09 code.[68] The computational cost of TDDFT calculations limited us to consider only the dimer model with 6-31G* basis. We have used different exchange-correlation functionals to check for the effect of exact exchange as well as the long-range nature of the functionals on the excitations. The lowest optical excitations with sizable oscillator strengths obtained with various exchange-correlation functionals are presented in Table 4. This excitation is generally a mixture of excitations from the HOMO and HOMO−1 to the LUMO and LUMO+1 orbitals. The excitation energies and the mixture of excitations depend heavily on the choice of exchange-correlation functional. The excitation energy extends over an energy range of nearly 0.6 eV. To qualitatively understand the effect of the exchange-correlation functionals, we also included the negative of the HOMO eigenvalue in Table 4 for the various functionals used here as a measure of the predicted ionization potential.

**Table 4. Comparison of Optical Transitions Predicted by TDDFT Using Various Functionals**

| functional | $-\varepsilon_{HOMO}$ (eV) | singlet | oscillator strength | excitations |
|---|---|---|---|---|
| PBE | 4.10 | 1.42 | 0.11 | H → L+1 (67%), H-1 → L+1 (19%), H-1 → L (6%), H → L (2%) |
| LC-BLYP | 6.58 | 2.12 | 0.44 | H-1 → L (74%), H-1 → L+1 (3%), H → L (12%), H → L+1 (8%) |
| CAM-B3LYP | 5.58 | 1.76 | 0.12 | H → L (72%), H → L+1 (24%) |
| LC-wPBE | 6.63 | 2.09 | 0.45 | H-1 → L+1 (3%), H-1 → L (67%), H → L (15%), H → L+1 (1%) |
| WB97 | 6.50 | 2.07 | 0.43 | H-1 → L (67%), H-1 → L+1 (4%), H → L (16%), H → L+1 (10%) |
| wB97XD | 6.15 | 1.87 | 0.22 | H-1 → L (3%), H → L (32%), H → L+1 (63%) |
| WB97x | 6.38 | 2.03 | 0.37 | H-1 → L (77%), H-1 → L+1 (3%), H → L (13%), H → L+1 (6%) |
| Expt. | 5.2 | 1.6 | | |

The long-range part of the functionals that are corrected to describe the charge transfer excitations can also improve the HOMO eigenvalues. It was found that the recent long-range corrected functionals give orbital energies in quantitative agreement with experiment for finite systems, mostly due to improved behavior of the functionals with the number of electrons.[69,70] We have noted that the HOMO eigenvalue of the dimer obtained from the PBE functional is lower than the theoretical value for the dimer, whereas the eigenvalues obtained with wB97, wB97XD, wB97X, LC-wPBE, and LC-BLYP are much higher (Table 4).[59,71−76] The CAM-B3LYP functional yields a value of 5.58 eV, which is closer to the experimental and theoretical value from Table 2.[77] This result shows that the asymptotic description of the exchange-correlation functional in the CAM-B3LYP is adequate to describe both the charge transfer excitations and the eigenvalues, and the optical excitation energies are in better agreement with the experimental values compared to the other functionals used here. Inclusion of exact exchange leads to better asymptotic behavior of the DFT potential. Earlier work by Sini et al. has shown that the inclusion of the exact exchange is crucial to obtain reliable properties such as HOMO−LUMO gaps and ground-state charge transfer for molecular crystals.[78]

## CONCLUSIONS

Co-crystals of organic semiconductors can reveal electronic donor−acceptor interactions in the solid state. We find that TIPS-Pn and F8TIPS-Pn can crystallize as an alloy from both bulk growth from solution and in blade-cast thin films. While the mixed crystalline phases of pentacene:perfluoropentacene blends are reportedly 1:1 stoichiometric mixtures, our data indicate that the structure of TIPS-Pn:F8TIPS-Pn mixed crystals changes continuously with increasing F8TIPS-Pn fraction.[45,51] Within experimental error, solution cast thin films of TIPS-Pn:F8TIPS-Pn do not show significant broadening of X-ray scattering peaks relative to neat films, which we attribute to the geometric similarity between the two compounds. Optical measurements of the mixed films reveal a red-shifted absorption edge relative to their constituents. The absorption spectra of mixed films cannot be fit to any linear combination of the parent films, indicating that there is little phase separation into pure components. While the photoluminescence quantum yield is low for these materials in the solid state, this system is a good candidate for study of charge generation methods such as transient absorption spectroscopy[79−81] or microwave conductivity.[82]

## ASSOCIATED CONTENT

### Supporting Information

The Supporting Information is available free of charge on the ACS Publications website at DOI: 10.1021/acs.jpcc.5b06363.

The supporting information includes experimental procedures, crystallographic data, optical spectra (PDF), and crystallographic data in CIF format.



DOI: 10.1021/acs.jpcc.5b06363
J. Phys. Chem. C 2015, 119, 20823−20832

## AUTHOR INFORMATION


### Corresponding Author

*E-mail: mchabinyc@engineering.ucsb.edu.


### Notes

The authors declare no competing financial interest.

## ACKNOWLEDGMENTS

J.S. and M.L.C. were supported by the Center for Energy Efficient Materials, an Energy Frontier Research Center funded by the U.S. Department of Energy, Office of Science, Office of Basic Energy Sciences under Award Number DE-SC0001009. T.B. and T.Z. were supported by the DOE Basic Energy Science under awards DE-SC0006818, DE-SC0002168 and the NSF PREM program between UCSB and UTEP (DMR-1205302). J.E.A. and B.P. were supported by the Office of Naval Research (N00014-11-1-0329). Authors thank the Texas Advanced Computing Center (TACC) from the National Science Foundation (NSF) (Grant No. TG-DMR090071) and NERSC for computational resources. This work made use of MRL Central Facilities supported by the MRSEC Program of the National Science Foundation under award No. DMR 1121053. Use of the Stanford Synchrotron Radiation Lightsource, SLAC National Accelerator Laboratory, is supported by the U.S. Department of Energy, Office of Science, Office of Basic Energy Sciences under Contract No. DE-AC02-76SF00515. We also thank Prof. Javier Read de Alaniz, Dr. Sameh Helmy and Dr. Gesine Veits (UCSB) for assistance with NMR and HPLC and Prof. Sahar Sharifzadeh for discussions on excitations in TIPS-Pn.

## REFERENCES


(1) Dou, L.; You, J.; Hong, Z.; Xu, Z.; Li, G.; Street, R. A.; Yang, Y. 25th Anniversary Article: A Decade of Organic/Polymeric Photovoltaic Research. *Adv. Mater.* **2013**, *25*, 6642−6671.

(2) Foster, R. Electron donor-acceptor complexes. *J. Phys. Chem.* **1980**, *84*, 2135−2141.

(3) Mulliken, R. S. Molecular Compounds and their Spectra. II. *J. Am. Chem. Soc.* **1952**, *74*, 811−824.

(4) Bendikov, M.; Wudl, F.; Perepichka, D. F. Tetrathiafulvalenes, Oligoacenenes, and Their Buckminsterfullerene Derivatives: The Brick and Mortar of Organic Electronics. *Chem. Rev.* **2004**, *104*, 4891−4946.

(5) Ferraris, J.; Cowan, D. O.; Walatka, V.; Perlstein, J. H. Electron transfer in a new highly conducting donor-acceptor complex. *J. Am. Chem. Soc.* **1973**, *95*, 948−949.

(6) Park, S. K.; Varghese, S.; Kim, J. H.; Yoon, S.-J.; Kwon, O. K.; An, B.-K.; Gierschner, J.; Park, S. Y. Tailor-Made Highly Luminescent and Ambipolar Transporting Organic Mixed Stacked Charge-Transfer Crystals: An Isometric Donor−Acceptor Approach. *J. Am. Chem. Soc.* **2013**, *135*, 4757−4764.

(7) Zhu, L.; Yi, Y.; Fonari, A.; Corbin, N. S.; Coropceanu, V.; Brédas, J.-L. Electronic Properties of Mixed-Stack Organic Charge-Transfer Crystals. *J. Phys. Chem. C* **2014**, *118*, 14150−14156.

(8) Zhu, L.; Yi, Y.; Li, Y.; Kim, E.-G.; Coropceanu, V.; Brédas, J.-L. Prediction of Remarkable Ambipolar Charge-Transport Characteristics in Organic Mixed-Stack Charge-Transfer Crystals. *J. Am. Chem. Soc.* **2012**, *134*, 2340−2347.

(9) Kitaigorodsky, A. I. *Mixed Crystals*; Softcover reprint of the original 1st ed. 1984.; Springer, 2012.

(10) Kuvadia, Z. B.; Doherty, M. F. Effect of Structurally Similar Additives on Crystal Habit of Organic Molecular Crystals at Low Supersaturation. *Cryst. Growth Des.* **2013**, *13*, 1412−1428.

(11) Shtukenberg, A. G.; Lee, S. S.; Kahr, B.; Ward, M. D. Manipulating Crystallization with Molecular Additives. *Annu. Rev. Chem. Biomol. Eng.* **2014**, *5*, 77−96.

(12) Berkovitch-Yellin, Z.; Van Mil, J.; Addadi, L.; Idelson, M.; Lahav, M.; Leiserowitz, L. Crystal morphology engineering by "tailor-made" inhibitors; a new probe to fine intermolecular interactions. *J. Am. Chem. Soc.* **1985**, *107*, 3111−3122.

(13) Kahr, B.; Gurney, R. W. Dyeing Crystals. *Chem. Rev.* **2001**, *101*, 893−952.

(14) Hogge, W. C. *Effect of HNS on physical properties of TNT explosives: surveillance evaluation*; NWSY-TR-79-1; Naval Weapons Station, 1979.

(15) Bolton, O.; Matzger, A. J. Improved Stability and Smart-Material Functionality Realized in an Energetic Cocrystal. *Angew. Chem., Int. Ed.* **2011**, *50*, 8960−8963.

(16) Landenberger, K. B.; Bolton, O.; Matzger, A. J. Two Isostructural Explosive Cocrystals with Significantly Different Thermodynamic Stabilities. *Angew. Chem., Int. Ed.* **2013**, *52*, 6468−6471.

(17) Anzenbacher, P.; Montes, V. A.; Takizawa, S. High-purity white light from a simple single dopant host-guest white organic light-emitting diode architecture. *Appl. Phys. Lett.* **2008**, *93*, 163302.

(18) Baldo, M. A.; Thompson, M. E.; Forrest, S. R. High-efficiency fluorescent organic light-emitting devices using a phosphorescent sensitizer. *Nature* **2000**, *403*, 750−753.

(19) Rosenstock, H. B. Luminescent Emission from an Organic Solid with Traps. *Phys. Rev.* **1969**, *187*, 1166−1168.

(20) Probst, K. H.; Karl, N. Energy Levels of Electron and Hole Traps in the Band Gap of Doped Anthracene Crystals. *Phys. Status Solidi A* **1975**, *27*, 499−508.

(21) Salzmann, I.; Duhm, S.; Heimel, G.; Rabe, J. P.; Koch, N.; Oehzelt, M.; Sakamoto, Y.; Suzuki, T. Structural Order in Perfluoropentacene Thin Films and Heterostructures with Pentacene. *Langmuir* **2008**, *24*, 7294−7298.

(22) Platt, A. D.; Day, J.; Subramanian, S.; Anthony, J. E.; Ostroverkhova, O. Optical, Fluorescent, and (Photo)conductive Properties of High-Performance Functionalized Pentacene and Anthradithiophene Derivatives. *J. Phys. Chem. C* **2009**, *113*, 14006−14014.

(23) Giri, G.; Verploegen, E.; Mannsfeld, S. C. B.; Atahan-Evrenk, S.; Kim, D. H.; Lee, S. Y.; Becerril, H. A.; Aspuru-Guzik, A.; Toney, M. F.; Bao, Z. Tuning charge transport in solution-sheared organic semiconductors using lattice strain. *Nature* **2011**, *480*, 504−508.

(24) Rivnay, J.; Noriega, R.; Kline, R. J.; Salleo, A.; Toney, M. F. Quantitative analysis of lattice disorder and crystallite size in organic semiconductor thin films. *Phys. Rev. B: Condens. Matter Mater. Phys.* **2011**, *84*, 045203.

(25) Anthony, J. E.; Vogel, D. E.; Schnobrich, S. M.; Clough, R. S.; Novack, J. C.; Redinger, D. Silylethyne-Substituted Pentacenes. *Mater. Matters* **2009**, *4*, 58.

(26) Swartz, C. R.; Parkin, S. R.; Bullock, J. E.; Anthony, J. E.; Mayer, A. C.; Malliaras, G. G. Synthesis and Characterization of Electron-Deficient Pentacenes. *Org. Lett.* **2005**, *7*, 3163−3166.

(27) Anthony, J. E.; Eaton, D. L.; Parkin, S. R. A Road Map to Stable, Soluble, Easily Crystallized Pentacene Derivatives. *Org. Lett.* **2002**, *4*, 15−18.

(28) Desiraju, G. R.; Gavezzotti, A. Crystal structures of polynuclear aromatic hydrocarbons. Classification, rationalization and prediction from molecular structure. *Acta Crystallogr., Sect. B: Struct. Sci.* **1989**, *45*, 473−482.

(29) Patrick, C. R.; Prosser, G. S. A Molecular Complex of Benzene and Hexafluorobenzene. *Nature* **1960**, *187*, 1021−1021.

(30) Williams, J. H.; Cockcroft, J. K.; Fitch, A. N. Structure of the Lowest Temperature Phase of the Solid Benzene−Hexafluorobenzene Adduct. *Angew. Chem., Int. Ed. Engl.* **1992**, *31*, 1655−1657.

(31) Cozzi, F.; Ponzini, F.; Annunziata, R.; Cinquini, M.; Siegel, J. S. Polar Interactions between Stacked $\pi$ Systems in Fluorinated 1,8-Diarylnaphthalenes: Importance of Quadrupole Moments in Molecular Recognition. *Angew. Chem., Int. Ed. Engl.* **1995**, *34*, 1019−1020.

(32) Wheeler, S. E.; Houk, K. N. Through-Space Effects of Substituents Dominate Molecular Electrostatic Potentials of Substituted Arenes. *J. Chem. Theory Comput.* **2009**, *5*, 2301−2312.




DOI: 10.1021/acs.jpcc.5b06363
J. Phys. Chem. C 2015, 119, 20823−20832

(33) Parrish, R. M.; Sherrill, C. D. Quantum-Mechanical Evaluation of $\pi-\pi$ versus Substituent$-\pi$ Interactions in $\pi$ Stacking: Direct Evidence for the Wheeler−Houk Picture. *J. Am. Chem. Soc.* **2014**, *136*, 17386−17389.
(34) Ponzini, F.; Zagha, R.; Hardcastle, K.; Siegel, J. S. Phenyl/Pentafluorophenyl Interactions and the Generation of Ordered Mixed Crystals: sym-Triphenethynylbenzene and sym-Tris-(perfluorophenethynyl)benzene. *Angew. Chem., Int. Ed.* **2000**, *39*, 2323−2325.
(35) Coates, G. W.; Dunn, A. R.; Henling, L. M.; Dougherty, D. A.; Grubbs, R. H. Phenyl−Perfluorophenyl Stacking Interactions: A New Strategy for Supermolecule Construction. *Angew. Chem., Int. Ed. Engl.* **1997**, *36*, 248−251.
(36) Sakamoto, Y.; Suzuki, T.; Kobayashi, M.; Gao, Y.; Fukai, Y.; Inoue, Y.; Sato, F.; Tokito, S. Perfluoropentacene: High-Performance p−n Junctions and Complementary Circuits with Pentacene. *J. Am. Chem. Soc.* **2004**, *126*, 8138−8140.
(37) Bondi, A. van der Waals Volumes and Radii. *J. Phys. Chem.* **1964**, *68*, 441−451.
(38) Approximate atomic volumes in cubic ångstroms.
(39) Pope, M. *Electronic Processes in Organic Crystals and Polymers*; in Monographs on the physics and chemistry of materials, 2nd ed.; Oxford University Press: New York, 1999.
(40) Goetz, K. P.; Vermeulen, D.; Payne, M. E.; Kloc, C.; McNeil, L. E.; Jurchescu, O. D. Charge-transfer complexes: new perspectives on an old class of compounds. *J. Mater. Chem. C* **2014**, *2*, 3065−3076.
(41) Mori, T.; Inokuchi, H. Structural and electrical properties of (BEDT-TTF) (TCNQ). *Solid State Commun.* **1986**, *59*, 355−359.
(42) Vermeulen, D.; Zhu, L. Y.; Goetz, K. P.; Hu, P.; Jiang, H.; Day, C. S.; Jurchescu, O. D.; Coropceanu, V.; Kloc, C.; McNeil, L. E. Charge Transport Properties of Perylene−TCNQ Crystals: The Effect of Stoichiometry. *J. Phys. Chem. C* **2014**, *118*, 24688−24696.
(43) Haas, S.; Batlogg, B.; Besnard, C.; Schiltz, M.; Kloc, C.; Siegrist, T. Large uniaxial negative thermal expansion in pentacene due to steric hindrance. *Phys. Rev. B: Condens. Matter Mater. Phys.* **2007**, *76*, 205203.
(44) Chen, J.; Martin, D. C.; Anthony, J. E. Morphology and molecular orientation of thin-film bis(triisopropylsilylethynyl) pentacene. *J. Mater. Res.* **2007**, *22*, 1701−1709.
(45) Hinderhofer, A.; Frank, C.; Hosokai, T.; Resta, A.; Gerlach, A.; Schreiber, F. Structure and morphology of coevaporated pentacene-perfluoropentacene thin films. *J. Chem. Phys.* **2011**, *134*, 104702.
(46) Mayer, A. C.; Kazimirov, A.; Malliaras, G. G. Dynamics of Bimodal Growth in Pentacene Thin Films. *Phys. Rev. Lett.* **2006**, *97*, 105503.
(47) Mannsfeld, S. C. B.; Tang, M. L.; Bao, Z. Thin Film Structure of Triisopropylsilylethynyl-Functionalized Pentacene and Tetraceno[2,3-b]thiophene from Grazing Incidence X-Ray Diffraction. *Adv. Mater.* **2011**, *23*, 127−131.
(48) Rivnay, J.; Mannsfeld, S. C. B.; Miller, C. E.; Salleo, A.; Toney, M. F. Quantitative Determination of Organic Semiconductor Microstructure from the Molecular to Device Scale. *Chem. Rev.* **2012**, *112*, 5488−5519.
(49) Sherman, J. B.; Purushothaman, B.; Parkin, S. R.; Kim, C.; Collins, S.; Anthony, J.; Nguyen, T.-Q.; Chabinyc, M. L. Role of crystallinity of non-fullerene acceptors in bulk heterojunctions. *J. Mater. Chem. A* **2015**, *3*, 9989−9998.
(50) Love, J. A.; Proctor, C. M.; Liu, J.; Takacs, C. J.; Sharenko, A.; van der Poll, T. S.; Heeger, A. J.; Bazan, G. C.; Nguyen, T.-Q. Film Morphology of High Efficiency Solution-Processed Small-Molecule Solar Cells. *Adv. Funct. Mater.* **2013**, *23*, 5019−5026.
(51) Haas, B.; Gries, K. I.; Breuer, T.; Häusler, I.; Witte, G.; Volz, K. Microstructural Characterization of Organic Heterostructures by (Transmission) Electron Microscopy. *Cryst. Growth Des.* **2014**, *14*, 3010−3014.
(52) Gelbrich, T.; Threlfall, T. L.; Hursthouse, M. B. XPac dissimilarity parameters as quantitative descriptors of isostructurality: the case of fourteen 4,5′-substituted benzenesulfonamido-2-pyridines obtained by substituent interchange involving CF3/I/Br/Cl/F/Me/H. *CrystEngComm* **2012**, *14*, 5454.
(53) Fabbiani, F. P. A.; Dittrich, B.; Florence, A. J.; Gelbrich, T.; Hursthouse, M. B.; Kuhs, W. F.; Shankland, N.; Sowa, H. Crystal structures with a challenge: high-pressure crystallisation of ciprofloxacin sodium salts and their recovery to ambient pressure. *CrystEngComm* **2009**, *11*, 1396−1406.
(54) Anger, F.; Ossó, J. O.; Heinemeyer, U.; Broch, K.; Scholz, R.; Gerlach, A.; Schreiber, F. Photoluminescence spectroscopy of pure pentacene, perfluoropentacene, and mixed thin films. *J. Chem. Phys.* **2012**, *136*, 054701.
(55) McConnell, H. M.; Hoffman, B. M.; Metzger, R. M. Charge Transfer in Molecular Crystals. *Proc. Natl. Acad. Sci. U. S. A.* **1965**, *53*, 46−50.
(56) Torrance, J. B.; Vazquez, J. E.; Mayerle, J. J.; Lee, V. Y. Discovery of a Neutral-to-Ionic Phase Transition in Organic Materials. *Phys. Rev. Lett.* **1981**, *46*, 253−257.
(57) Piliego, C.; Loi, M. A. Charge transfer state in highly efficient polymer−fullerene bulk heterojunction solar cells. *J. Mater. Chem.* **2012**, *22*, 4141.
(58) Verlaak, S.; Beljonne, D.; Cheyns, D.; Rolin, C.; Linares, M.; Castet, F.; Cornil, J.; Heremans, P. Electronic Structure and Geminate Pair Energetics at Organic−Organic Interfaces: The Case of Pentacene/$C_{60}$ Heterojunctions. *Adv. Funct. Mater.* **2009**, *19*, 3809−3814.
(59) Perdew, J. P.; Burke, K.; Ernzerhof, M. Generalized Gradient Approximation Made Simple. *Phys. Rev. Lett.* **1996**, *77*, 3865−3868.
(60) Pederson, M. R.; Jackson, K. A. Variational mesh for quantum-mechanical simulations. *Phys. Rev. B: Condens. Matter Mater. Phys.* **1990**, *41*, 7453−7461.
(61) Jackson, K.; Pederson, M. R. Accurate forces in a local-orbital approach to the local-density approximation. *Phys. Rev. B: Condens. Matter Mater. Phys.* **1990**, *42*, 3276−3281.
(62) Pederson, M. R.; Jackson, K. A. Pseudoenergies for simulations on metallic systems. *Phys. Rev. B: Condens. Matter Mater. Phys.* **1991**, *43*, 7312−7315.
(63) Porezag, D.; Pederson, M. R. Infrared intensities and Raman-scattering activities within density-functional theory. *Phys. Rev. B: Condens. Matter Mater. Phys.* **1996**, *54*, 7830−7836.
(64) Porezag, D.; Pederson, M. R. Optimization of Gaussian basis sets for density-functional calculations. *Phys. Rev. A: At., Mol., Opt. Phys.* **1999**, *60*, 2840−2847.
(65) Jackson, K.; Yang, M.; Jellinek, J. Site-Specific Analysis of Dielectric Properties of Finite Systems. *J. Phys. Chem. C* **2007**, *111*, 17952−17960.
(66) Weinhold, F.; Carpenter, J. E. *The Structure of Small Molecules and Ions*; Naaman, R., Vager, Z., Eds.; Plenum, 1988.
(67) Dapprich, S.; Frenking, G. Investigation of Donor-Acceptor Interactions: A Charge Decomposition Analysis Using Fragment Molecular Orbitals. *J. Phys. Chem.* **1995**, *99*, 9352−9362.
(68) Frisch, M. J.; Trucks, G. W.; Schlegel, H. B.; Scuseria, G. E.; Robb, M. A.; Cheeseman, J. R.; Scalmani, G.; Barone, V.; Mennucci, B.; Petersson, G. A.; et al. *Gaussian 09*; Gaussian, Inc.
(69) Cohen, A. J.; Mori-Sánchez, P.; Yang, W. Fractional charge perspective on the band gap in density-functional theory. *Phys. Rev. B: Condens. Matter Mater. Phys.* **2008**, *77*, 115123.
(70) Tsuneda, T.; Song, J.-W.; Suzuki, S.; Hirao, K. On Koopmans' theorem in density functional theory. *J. Chem. Phys.* **2010**, *133*, 174101.
(71) Chai, J.-D.; Head-Gordon, M. Long-range corrected hybrid density functionals with damped atom-atom dispersion corrections. *Phys. Chem. Chem. Phys.* **2008**, *10*, 6615−6620.
(72) Chai, J.-D.; Head-Gordon, M. Systematic optimization of long-range corrected hybrid density functionals. *J. Chem. Phys.* **2008**, *128*, 084106.
(73) Vydrov, O. A.; Scuseria, G. E. Assessment of a long-range corrected hybrid functional. *J. Chem. Phys.* **2006**, *125*, 234109.
(74) Vydrov, O. A.; Heyd, J.; Krukau, A. V.; Scuseria, G. E. Importance of short-range versus long-range Hartree-Fock exchange for the performance of hybrid density functionals. *J. Chem. Phys.* **2006**, *125*, 074106.


DOI: 10.1021/acs.jpcc.5b06363
*J. Phys. Chem. C* 2015, 119, 20823−20832

(75) Iikura, H.; Tsuneda, T.; Yanai, T.; Hirao, K. A long-range correction scheme for generalized-gradient-approximation exchange functionals. *J. Chem. Phys.* **2001**, *115*, 3540.
(76) Vydrov, O. A.; Scuseria, G. E.; Perdew, J. P. Tests of functionals for systems with fractional electron number. *J. Chem. Phys.* **2007**, *126*, 154109.
(77) Yanai, T.; Tew, D. P.; Handy, N. C. A new hybrid exchange-correlation functional using the Coulomb-attenuating method (CAM-B3LYP). *Chem. Phys. Lett.* **2004**, *393*, 51−57.
(78) Sini, G.; Sears, J. S.; Brédas, J.-L. Evaluating the Performance of DFT Functionals in Assessing the Interaction Energy and Ground-State Charge Transfer of Donor/Acceptor Complexes: Tetrathiafulvalene−Tetracyanoquinodimethane (TTF−TCNQ) as a Model Case. *J. Chem. Theory Comput.* **2011**, *7*, 602−609.
(79) Gélinas, S.; Rao, A.; Kumar, A.; Smith, S. L.; Chin, A. W.; Clark, J.; van der Poll, T. S.; Bazan, G. C.; Friend, R. H. Ultrafast Long-Range Charge Separation in Organic Semiconductor Photovoltaic Diodes. *Science* **2014**, *343*, 512−516.
(80) Sharifzadeh, S.; Wong, C. Y.; Wu, H.; Cotts, B. L.; Kronik, L.; Ginsberg, N. S.; Neaton, J. B. Relating the Physical Structure and Optoelectronic Function of Crystalline TIPS-Pentacene. *Adv. Funct. Mater.* **2015**, *25*, 2038−2046.
(81) Wong, C. Y.; Cotts, B. L.; Wu, H.; Ginsberg, N. S. Exciton dynamics reveal aggregates with intermolecular order at hidden interfaces in solution-cast organic semiconducting films. *Nat. Commun.* **2015**, *6*, 5946.
(82) Wakamiya, A.; Nishimura, H.; Fukushima, T.; Suzuki, F.; Saeki, A.; Seki, S.; Osaka, I.; Sasamori, T.; Murata, M.; Murata, Y.; et al. On-Top $\pi$-Stacking of Quasiplanar Molecules in Hole-Transporting Materials: Inducing Anisotropic Carrier Mobility in Amorphous Films. *Angew. Chem., Int. Ed.* **2014**, *53*, 5800−5804.



DOI: 10.1021/acs.jpcc.5b06363
*J. Phys. Chem. C* 2015, 119, 20823−20832